5) The assumption of thermodynamic equilibrium for the analysis of fluctuation effects is more applicable at very high temperatures.

6) The application of this method of analysis for re-entry flight conditions requires an estimate of the temperature fluctuation magnitudes, statistical distribution function, and optimum autocorrelation which are presently not available from experimental measurements.

References

[1] Wallace, J., *Hypersonic Turbulent Boundary Layer Measurements Using an Electron Beam*, NASA SP-216, Dec. 10–11, 1968, p. 255.

[2] Kistler, A., "Fluctuation Measurements in a Supersonic Turbulent Boundary Layer," *The Physics of Fluids*, Vol. 2, No. 3, 1959, p. 290.

[3] Demetriades, A., "Electron Fluctuations in an Equilibrium Turbulent Plasma," *AIAA Journal*, Vol. 2, No. 7, July 1964, pp. 1347–1349; also Lane, F. and Zeiberg, S. L., "Comment on 'Electron Fluctuation in an Equilibrium Turbulent Plasma,'" *AIAA Journal*, Vol. 3, No. 5, May 1965, pp. 989–990.

[4] Kubert, B., "The Computation of the Products of Chemical Reactions in Equilibrium," TR U-1721, 1961, Philco-Ford, Calif.

[5] Bortner, M., "A Review of Rate Constants of Reactions in Re-entry Flow Fields," T15 R685D13, June 1968, General Electric.

[6] Kane, J., "Nonequilibrium Sodium Ionization in Laminar Boundary Layers," *AIAA Journal*, Vol. 2, No. 9, Sept. 1964, pp. 1651–1653.

[7] Favre, A., "Review of Space-Time Correlations in Turbulent Fluids," *Journal of Applied Mechanics*, June 1965, p. 241.

AUGUST 1971 AIAA JOURNAL VOL. 9, NO. 8

Fluid Mechanics of Train-Tunnel Systems in Unsteady Motion

MIKLOS SAJBEN*
California Institute of Technology, Pasadena, Calif.

The dynamic characteristics of bodies moving in long, finite channels are studied using a one-dimensional, incompressible fluid description. It is shown that the motion of the body and the fluid contained in the channel are closely and nonlinearly coupled and therefore an understanding of the system dynamics requires consideration of both body and fluid. The nonsteady inertial aspects of the motion may be important in many practical situations. The character of the solution is investigated using phase plane methods. The findings are compared with numerically integrated solutions yielding body and fluid speeds, as well as drag coefficients. The effects of various initial body speeds are studied. Compressibility effects are estimated and found to be slight for present systems. The theory includes steady-state operation as a singular case.

Nomenclature

c_D = drag coefficient
D = drag force on body
f = friction coefficient
F = propulsive force
k_j = loss coefficients defined in Eq. (18), j = 1 to 5
l = body length
L = channel length
m_j = loss coefficients defined in Eq. (24), j = 3 to 5
M = body mass; Mach number
p = static pressure
P = propulsion power
r = radial coordinate
R = channel or body radius
Re = Reynolds number
t = time
u = air velocity
U = mean air velocity
V = body velocity
x = coordinate along channel axis
X = body position coordinate
β = U/V velocity ratio
ϕ = $(\kappa_c/\kappa_b)^{1/2}$
γ = ratio of specific heats
Δ = distance of near field boundary from parallel section of body
ν = kinematic viscosity
κ = loss coefficient
λ = characteristic length
ψ = $L\rho R_c^2\pi/M$, air to body mass ratio
ρ = fluid density
σ = $(R_b/R_c)^2$, blockage ratio
ξ = axial coordinate in coordinate system fixed to body
ζ = loss coefficient

Subscripts

b = body
c = channel
cr = critical
e = exit
f,F = locations deffned on Fig. 2
0 = inlet
r,R = locations defined on Fig. 2
1,2 = locations defined on Fig. 1
$*$ = steady-state

Superscripts

$\pm$ = $U \gtrless 0$
$\hat{}$ = modified value (Eqs. 12, 27, and 33)

Presented as Paper 70-141 at the AIAA 8th Aerospace Sciences Meeting, New York, January 19–21, 1970; submitted August 12, 1970; revision received April 28, 1971. The author wishes to express his appreciation to B. Dayman, Jr., and to T. Kubota for numerous interesting discussions and useful comments on this subject. The interest and support of L. Lees is gratefully acknowledged.

* Presently Associate Scientist at McDonnell Douglas Research Laboratories, St. Louis, Mo. Member AIAA.

1. Introduction

SUBWAY systems presently under consideration are intended to employ higher speeds and higher traffic densities than systems in operation today. Both factors tend to aggravate problems of aerodynamic nature: the additional power requirement due to air drag is higher, the heat released

by the propulsion machinery of the train is more and the passenger discomfort due to air blast at the stations is also likely to increase.

In order to take these factors into account in the process of engineering design, one must be able to predict the drag as well as the air speed in the tunnel quantitatively. At the present, it is not entirely understood just what are the most important parameters influencing these two quantities.

The present study presents a theory describing the dynamic behavior of systems consisting of a train and the air confined in a tunnel. The air is assumed to be incompressible and the description is one-dimensional. The formulation admits time-dependent, unsteady operation, which includes steady-state as the special case of vanishing time derivatives. It is shown that the motion of the train and the motion of the air in the tunnel are intimately coupled and one cannot adequately describe either without considering the other. It is also shown that the train-air system may very well move in a nonstationary fashion for a large fraction of its operational time. This implies power requirements considerably in excess of those calculated by assuming stationary motion in the system.

Section 2 is devoted to the formulation of a model reasonably representative of near-future applications. In Sec. 3 the governing equations are derived. Analysis of these equations in Sec. 4 reveals the main features of these solutions. In Sec. 5 numerically obtained solutions are presented and discussed, while comments on the limitations of the present theory are offered in Sec. 6.

2. Formulation of a One-Dimensional Model

We shall consider the motion of a long, cylindrical body constrained to move coaxially inside a long channel of constant, circular cross section (Fig. 1). The motion of the body is initiated and maintained by some propulsive force F acting between the body and the tunnel wall, exemplified by friction between train wheels and rails. In general, this propulsive force is related to the speed of the body in some manner determined by the force-speed characteristic of the propulsion units (torque-speed in the case of conventional rotating machines), so that it is appropriate to consider F as a function of body speed, V. Aerodynamic means of propulsion (propellers, rockets) will not be considered.

The channel is of finite length, L, terminated at both ends by constant pressure reservoirs, which need not be at the same pressure. In case of a full-size train, a tunnel is of course usually terminated in the outside atmosphere so that the end pressures are equal, but this is not necessarily the case in an experimental arrangement.

The fluid in the channel is assumed to be incompressible, which places limitations on the present theory in terms of allowable body speeds and the length of the channel. These will be discussed in Sec. 6.

Figure 1 shows a schematic of the channel-body system considered, indicating the relevant geometrical parameters. In particular, x is the position coordinate in the coordinate system fixed to the channel, defined positive in the direction of V.

We shall assume, as done before by Hara,[1] Hammitt[2] and others, that the flow in the channel is reasonably parallel up to within several channel diameters to the body and therefore can be adequately described by cross section averaged velocities and a similarly averaged pressure. This region will be called the "far field" which includes a downstream portion $x_1 < x < x_R$ and the upstream portion $x_F < x < x_2$. The region $x_R < x < x_F$ which includes the body, will clearly include regions of large radial velocities near the forward and rear stagnation points and will require separate treatment. It will be called the "near field" and discussed in terms of a body fixed coordinate system, whose origin is chosen at the foremost point of the body and whose axial coordinate is designated ξ (Fig. 2).

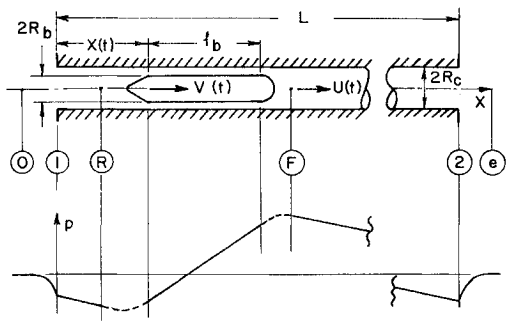

Fig. 1 Sketch of body-channel system. Lower part of graph illustrates instantaneous static pressure distribution for $p_e - p_0 = 0$.

The one-dimensional equations governing the space and time-dependent average fluid velocity and pressure in the far field are:

$$\partial u/\partial x = 0 \tag{1}$$

$$\partial u/\partial t = -1/\rho(\partial p/\partial x) - f_c/R_c\, u|u| \tag{2}$$

where f_c is a friction factor defined by

$$f_c \equiv \tau_c/(\tfrac{1}{2}\rho u^2)$$

where τ_c is the shear stress on the channel wall. The last term of Eq. (2) reflects the rather reasonable assumption that friction gives rise to a force that always opposes the mean velocity. While not true in regions of separated flow, it is nevertheless expected to be the case throughout the entire far field. f_c can be estimated from fully developed channel flow formulas,[3] or can also be determined by solving the appropriate (mostly turbulent) equations of motion in their axial symmetric, time-dependent form, although this approach is not likely to be practical. In what follows, we shall assume that f_c is a known function of the Reynolds number based on channel diameter and the mean air speed: $Re_c = 2R_cU/\nu$, where ν is the kinematic viscosity. If Re_c is very large, as is usually the case, then f_c becomes a very slowly varying function of Re_c and may conveniently be taken as constant. In this case f_c is primarily dependent on the surface roughness of the channel.[3]

Equations (1) and (2) can be obtained rigorously by integrating the equations of motion with respect to r over the range $0 \leq r \leq R_c$. The exact form shows that Eqs. (1) and (2) are valid if the shape of the velocity profile is independent of x and if the mean velocity u is interpreted as a displacement-

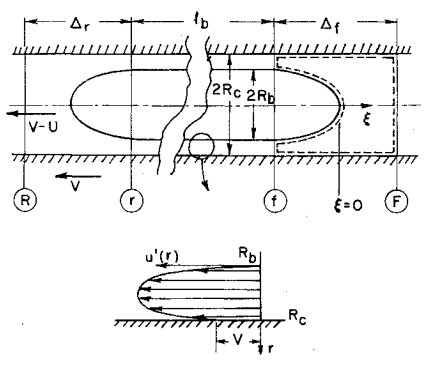

Fig. 2 Sketch of near-field dimensions and velocities in a coordinate system fixed to the body. Dashed line indicates control volume used to determine D_{fF}.

mean value defined by

$$u(x,t) = \frac{1}{R_c^2\pi}\int_0^{Rc} u'(x,r,t)2\pi r dr \tag{3}$$

where u' is the velocity as function of x, r and t.

The situation is more complex in the near field, where Eqs. (1) and (2) clearly do not apply. It is nevertheless possible to derive approximate relations between the overall pressure difference $(p_F - p_R)$, the velocities, U, V, and body drag by using the integral momentum theorem, as will be shown in Sec. 3. These relations are effectively one-dimensional and can be matched up satisfactorily with the description of the far field, so that a one-dimensional description of the entire system is possible.

The analysis of the near field is greatly simplified by the fact that the flow in this region can and will be treated as steady. The justification for this assumption lies in the fact that the time required by the near-field flow to adjust to steady-state after a perturbation of the $p_F - p_R$ pressure difference is much shorter than the time required by the entire system to reach steady-state after a perturbation of reservoir pressures or of propulsive force. This is intuitively quite likely if one considers that the first process involves only the mass of fluid in the near-field region, while the second process is governed by the inertia of all the fluid contained in the channel as well as the inertia of the body itself.

For simplicity, we shall restrict the discussion to cases where the near field is completely contained within the tube. Transient effects associated with the passage of the body through the channel inlet or exit can be easily treated with methods employed here.

The present one dimensional formulation contains two principal unknowns: the body velocity V, and the channel airspeed U. Two ordinary differential equations describing the time-wise variation of each will be derived in the next section. Both are found to be of first order, strongly coupled in a nonlinear fashion. The formulation includes the steady motion of the body as a singularity in the system of equations. Since steady-state operation has been discussed by Hara[1] in the one-dimensional approximation, we shall discuss it only to the extent necessary to make the present paper self contained.

3. Derivation of Governing Equations

The differential equation governing U is based on the axial momentum equation for the fluid. Equation (2) expresses this principle in a form valid for the far field, while the near field has to be treated separately. The two fields are matched by requiring the pressure and average velocity to be continuous at both x_R and x_F. The matching of pressures allows us to break down the (specified) overall pressure difference $(p_e - p_0)$ into several contributions as follows:

$$p_e - p_0 = (p_e - p_2) + (p_2 - p_F) + (p_F - p_R) + (p_R - p_1) + (p_1 - p_0) \tag{4}$$

The $(p_F - p_R)$ term on the right hand side characterizes the near field, the $(p_2 - p_F)$ and $(p_R - p_1)$ terms represent the far field while the remaining two terms correspond to inlet and exit flows. If we express all contributions in terms of U, V, and/or their time derivatives, Eq. (4) will become one of the equations required to formulate our problem properly. Accordingly, we shall now proceed to derive appropriate expressions for each of the pressure differences on the right hand side of Eq. (4).

Between stations 0 and 1 the velocity is a rapidly growing function of x, so that the $u\partial u/\partial x$ term dominates both $\partial u/\partial t$ and the friction term in the x momentum equation. Under these circumstances it is reasonable to express the inlet pressure drop as an empirical coefficient (ζ_0) times the inviscid pressure drop, as calculated from Bernoulli's equation:

$$\frac{p_1 - p_0}{\rho} = \frac{\zeta_0}{2}(u_0^2 - u_1^2) \approx -\tfrac{1}{2}\zeta_0 U^2 \tag{5}$$

since $u_1 \equiv u(x_1) = U$ by definition and $u_0 \ll u_1$. $\zeta_0 = 1$ for the truly inviscid case and should only be slightly larger for real inlets.

By Eq. (1), the air velocity U is independent of x throughout the far field. This fact allows us to integrate x out from Eq. (2). Integrating from x_1 to $x_R(t)$, we have

$$\frac{p_R - p_1}{\rho} = -\int_{x_1}^{x_R(t)}\left(\frac{\partial u}{\partial t} + \frac{f_c}{R_c}u|u|\right)dx \tag{6}$$

Using Leibnitz' rule, we deduce, after some manipulations:

$$\frac{p_R - p_1}{\rho} = -\frac{\partial}{\partial t}[U(x_R - x_1)] - \frac{f_c}{R_c}(x_R - x_1)U|U| + UV \tag{7}$$

where we used the assumption that x_R is a fixed distance behind the body and hence

$$dx_R/dt = dX/dt = V \tag{8}$$

The upstream portion of the far field is treated similarly, resulting in

$$\frac{p_2 - p_F}{\rho} = -\frac{\partial}{\partial t}[U(x_2 - x_F)] - \frac{f_c}{R_c}(x_2 - x_F)U|U| - UV \tag{9}$$

The fluid leaving the channel at x_2 carries considerable kinetic energy with it, most of which is dissipated in the jet formed by the exhaust. Introducing an exit loss coefficient ζ_e, we can write, analogously to Eq. (5):

$$\frac{p_e - p_2}{\rho} \simeq \tfrac{1}{2}\zeta_e U^2 \tag{10}$$

where $\zeta_e = 1$ for inviscid flow, and is expected to be considerably less for real exits. Substituting Eqs. (5–10) into Eq. (4) we have:

$$\frac{p_e - p_0}{\rho} = -\hat{L}\frac{dU}{dt} - \frac{f_c}{R_c}\hat{L}\langle U\rangle^2 - \tfrac{1}{2}(\zeta_0^{\pm} - \zeta_e^{\pm})U^2 + \frac{p_F - p_R}{\rho} \tag{11}$$

where

$$\hat{L} = L - (l_b + \Delta_R + \Delta_F) \tag{12}$$

is an effective channel length and Δ_R, Δ_F are each several channel radii long, the exact length being of little importance. The notation $\langle Z\rangle^2$ serves to abbreviate $Z|Z|$.

The $\pm$ superscript of the loss coefficients accounts for the fact that U is allowed to be either positive or negative, hence the channel ends may serve as either inlets or exits. Since the loss coefficients for the same end may be grossly different for the two cases, ζ_0^+ is understood to mean the loss coefficient for the $x = 0$ end if $U > 0$, while ζ_0^- applies to the same end if $U < 0$. Analogously, ζ_e^+ is the loss coefficient for the $x = L$ end if $U > 0$ while ζ_e^- is to be used for the $U < 0$. If the two ends of the tube are geometrically similar, then $\zeta_0^+ = \zeta_e^-$ and $\zeta_0^- = \zeta_e^+$. This fact may be used to simplify some of the equations that follow.

We now turn our attention to the near field region, in particular to the $p_R - p_F$ pressure difference appearing in Eq. (11). As mentioned before, the flow will be treated as steady in the reference frame fixed to the body.

First we break down $p_F - p_R$ into three parts as follows (see Fig. 2):

$$p_F - p_R = (p_F - p_f) + (p_f - p_r) + (p_r - p_R) \tag{13}$$

The locations of ξ_r and ξ_f are determined by requiring that the flow between them be essentially parallel, so that fully developed channel flow may be assumed over the range $\xi_r \leq \xi \leq \xi_f$.

We shall neglect viscous forces in the rapidly accelerating flow for $\xi_f \leq \xi \leq \xi_F$, as we have done for the inlet region of the tunnel. We can then again apply Bernoulli's equation and write

$$\frac{p_F - p_f}{\rho} = \tfrac{1}{2}\xi_F^{\pm}\left[\frac{1}{(1-\sigma)^2} - 1\right](V - U)^2 \qquad (14)$$

where σ is the blockage ratio defined as $(R_b/R_c)^2$, and $\zeta_F^{\pm}$ is an empirical loss coefficient, whose value depends on the sign of $(V - U)$, in complete analogy to the $\zeta_0^{\pm}$ coefficient. Note that $\zeta_F^{\pm} \geq 1$.

Next we consider an annular, cylindrical control volume enclosing all fluid in the region $\xi_f \leq \xi \leq \xi_f$ and apply the momentum integral theorem. The shear stress acting on each wall is assumed to be given by a product of an appropriate friction factor, the density halved, and the square of the relative speed between the mean flow and the respective wall. Since in the body-fixed frame the channel wall moves to the left with velocity V, the two relative speeds are not the same. Taking into account the direction of the shear forces, we can deduce:

$$\frac{p_f - p_r}{\rho} = -\frac{f_b l_b}{R_c}\frac{\sigma^{1/2}}{(1-\sigma)^3}\langle V - U\rangle^2 + \frac{f_c' l_b}{R_c}\frac{1}{(1-\sigma)^3}\langle \sigma V - U\rangle^2 \qquad (15)$$

where f_b refers to the body and f_c' to the channel surface in the near field.

The $p_r - p_R$ pressure drop depends on the details of the complex wake flow and presumably is strongly influenced by the shape of the body tail. Instead of considering all details, we simply assume the pressure recovery to be some empirical factor times the inviscid pressure difference:

$$\frac{p_r - p_R}{\rho} = -\tfrac{1}{2}\zeta_R^{\pm}\left[\frac{1}{(1-\sigma)^2} - 1\right](V - U)^2 \qquad (16)$$

where $\zeta_R^{\pm} \leq 1$. A more accurate value has to be determined by experiment. If $\zeta_R^{\pm}$ turns out to have a strong influence on the $V(t)$ or $U(t)$ behavior, then a more careful study is justified, otherwise this approximation will suffice.

Summing up Eqs. (14) to (16) yields an expression for $p_F - p_R$, which may be substituted into Eq. (11) to produce the equation governing $U(t)$:

$$\hat{L}\frac{dU}{dt} = -\frac{p_e - p_0}{\rho} - k_1\langle U\rangle^2 - k_2^{\pm}U^2 + k_3\langle V - U\rangle^2 + k_4\langle \sigma V - U\rangle^2 + k_5^{\pm}(V - U)^2 \qquad (17)$$

where the coefficients k_j are defined as

$$\begin{aligned} k_1 &= f_c\hat{L}/R_c \\ k_2^{\pm} &= \tfrac{1}{2}(\zeta_0^{\pm} - \zeta_e^{\pm}) \\ k_3 &= f_b l_b/R_c\sigma^{1/2}(1-\sigma)^{-3} \\ k_4 &= f_c' l_b/R_c(1-\sigma)^{-3} \\ k_5 &= \tfrac{1}{2}\sigma(2-\sigma)(1-\sigma)^{-2}(\zeta_F^{\pm} - \zeta_R^{\pm}) \end{aligned} \qquad (18)$$

Equation (17) is clearly quite general, since it is applicable to positive or negative air velocities as well as to nonzero pressure differences between the two channel ends.

Equation (17) needs to be complemented by a second equation governing $V(t)$. This is obtained by applying Newton's second law to the body:

$$M(dV/dt) = F(V) - D(V,U) \qquad (19)$$

where M is the mass of the body and D is the aerodynamic drag acting on it, including contributions due to both shear and normal stresses, i.e., both viscous and pressure drag. D is defined positive if it opposes the direction of V. D is expected to depend on both U and V in a manner derivable from considerations similar to those utilized so far.

We shall split the total drag into three contributions: 1) the drag acting on the nose region $\xi_f \leq \xi$; 2) the drag in the constant area middle region, $\xi_r \leq \xi \leq \xi_f$; and 3) the tail drag $\xi \leq \xi_r$. Each contribution can be determined by an application of the integral momentum theorem to a control volume, including all the fluid in the respective range of ξ, together with the equation of continuity and the already introduced definitions for the loss coefficients $\zeta_F^{\pm}$ and $\zeta_R^{\pm}$.

In the rapidly accelerating nose region flow we can apply Bernoulli's theorem, combined with the definition of the empirical loss coefficient [Eq. (14)], and obtain

$$\frac{D_{fF}}{R_c^2\pi} = \sigma\left[p_F - \frac{\rho}{2}\frac{2(1-\zeta_F^{\pm}) + \zeta_F^{\pm}\sigma}{1-\sigma}(V - U)^2\right] \qquad (20)$$

In the constant area middle region the drag is due solely to shear and is given by

$$\frac{D_{rf}}{R_c^2\pi} = f_b\frac{l_b}{R_c}\frac{\sigma^{1/2}}{(1-\sigma)^2}\rho\langle V - U\rangle^2 \qquad (21)$$

In the tail region, again the definition of the wake loss coefficient [Eq. (16)] provides a relation needed to determine the drag. The result is

$$\frac{D_{Rr}}{R_c^2\pi} = -\sigma\left[p_R - \frac{\rho}{2}\frac{2(1-\zeta_R^{\pm}) + \zeta_R^{\pm}\sigma}{1-\sigma}(V - U)^2\right] \qquad (22)$$

Equations (20) and (22) clearly neglect shear on the channel wall, consistently with Eqs. (14) and (16). A rough estimate shows that the ratio of wall shear force to the force due to static pressure change between locations f and F is approximately equal to $(2f\Delta/R_c)(1 - U/V)$, hence usually much less than one. This estimate points out that the wall will be dominant only if U/V is near unity, i.e., if the fluid speed relative to the body is nearly zero. This situation may arise if the body is being retarded by F (braking), which usually happens only temporarily. It is also worth noting that in most cases the shear on the channel wall changes sign between f and F, so that the contributions partially cancel. For these reasons, the admittedly crude representation of this loss through the use of an empirical loss coefficient will be considered adequate for the present purposes.

The total drag is obtained by summing the three contributions, leading to

$$\frac{D}{R_c^2\pi} = \sigma(p_F - p_R) + f_b\frac{l_b}{R_c}\frac{\sigma^{1/2}}{(1-\sigma)^2}\rho\langle V - U\rangle^2 + \frac{\sigma(2-\sigma)}{2(1-\sigma)}(\zeta_F^{\pm} - \zeta_R^{\pm})\rho(V - U)^2 \qquad (23)$$

Using Eqs. (14–16) to eliminate $p_F - p_R$, we obtain the differential equation governing V in the form

$$\frac{M}{\rho R_c^2\pi}\frac{dV}{dt} = \frac{F}{\rho R_c^2\pi} - m_3\langle V - U\rangle^2 - m_4\sigma\langle \sigma V - U\rangle^2 - m_5^{\pm}(V - U)^2 \qquad (24)$$

where the m_j coefficients are found to be exactly equal to the corresponding k_j coefficients appearing in Eq. (17): $m_j = k_j$, for $j = 3,4,5$. This fact is not surprising, since these three terms jointly express the aerodynamic drag which clearly must enter the equation for V.

By adding Eqs. (17) and (24), an alternate form for either equation may be obtained in which the expressions for drag

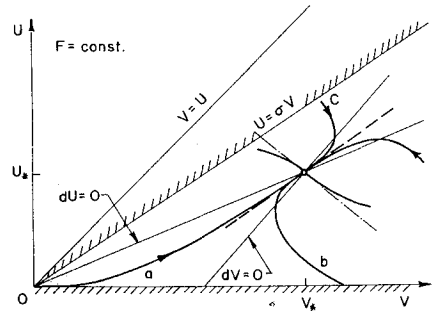

Fig. 3 $U(V)$ Phase plane with sample trajectories. Cross-hatched boundaries denote region of validity of simplified model.

cancel out almost completely. It can be written as follows:

$$F = M\frac{dV}{dt} + (\rho\hat{L}R_c^2\pi)\frac{dU}{dt} + \rho R_c^2\pi[k_1\langle U\rangle^2 + k_2^{\pm}U^2] + (p_e - p_0)R_c^2\pi - k_4\pi R_c^2(1-\sigma)\rho\langle\sigma V - U\rangle^2 \quad (25)$$

This form clearly shows the fact that the propulsion force acting on the body must overcome the inertia of the body itself, the inertia of the fluid in the channel, plus the frictional and inlet-exit losses of the channel flow, as represented by the U^2 terms. A nonzero pressure difference across the channel acts as an additional propulsive (or braking) force. The last term arises because the shear force acting on the body in the constant area section of the near field is not equal to the shear acting on the fluid in the same section. This term is usually small and of little importance.

Equations (17) and (24) represent two coupled, nonlinear differential equations that describe the behavior of our system for all possible initial conditions. In their present form they apply to a variety of practical situations. They describe the behavior of a train in a tunnel whether accelerating or decelerating, steady-state being also included as a special case when both derivatives vanish. The air velocity in the tunnel may be more or less than the velocity of the train, or it may even be negative as if generated by another train previously traversing the tunnel in the opposite direction.

4. The Character of Solutions

In the interest of simplifying further discussions and to permit analytical study of the equations, we shall make several

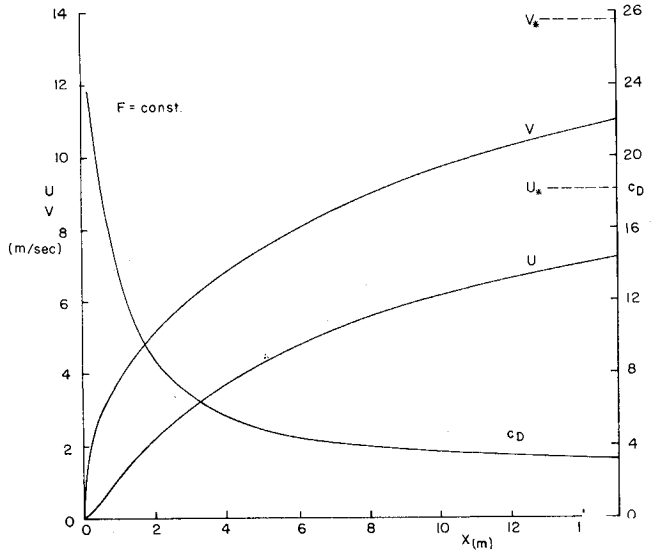

Fig. 4 Variation of V, U, and c_D as functions of body position for $V_0 = U_0 = 0$. Steady-state velocities indicated by dashed lines.

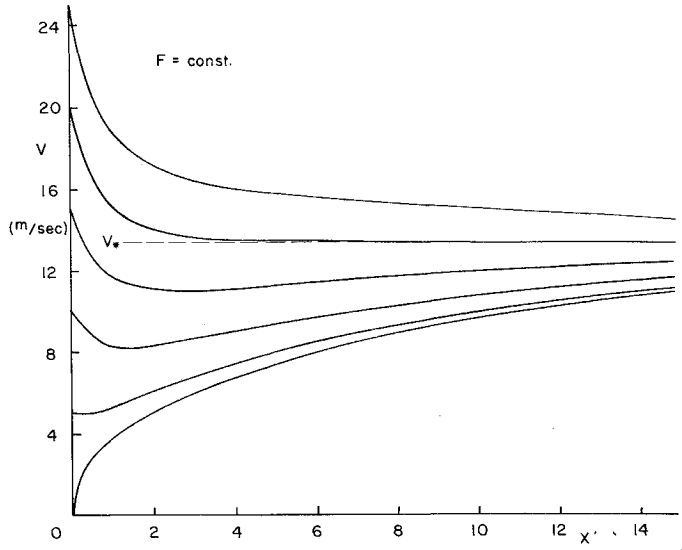

Fig. 5 Variation of V along channel for different initial body velocities ($U_0 = 0$). Steady-state velocity indicated with dashed line.

assumptions. First, we shall set $p_e - p_0 = 0$, corresponding to situations in which both ends of the channel are exposed to the atmosphere. If the fluid motion in the channel is induced by the body itself (as is almost invariably the case), then $U > 0$. We shall also make the often applicable restriction that $\sigma V \geq U$. The last two assumptions obviate the need for nonanalytic functions appearing in Eq. (17) and (24), without damaging the applicability of the theory to the most frequent train-tunnel problems.

Furthermore, we shall focus our attention on large blockage ratios. If σ is near one, then $\sigma V - U \sim V - U$ and the three terms expressing the drag in Eqs. (17) and (24) may be all lumped together into one single term proportional to $(V - U)^2$. The resulting set of governing equations is:

$$\hat{L}(dU/dt) = -(\kappa_c/2)U^2 + \kappa_b/2(V-U)^2 \quad (26)$$

$$\hat{L}/\psi(dV/dt) = \hat{F}(V) - \kappa_b/2(V-U)^2 \quad (27)$$

where κ_c and κ_b are again dimensionless coefficients given by $\kappa_c = 2(k_1 + k_2)$, $\kappa_b = 2(k_3 + k_4 + k_4) \simeq 2(m_3 + \sigma m_4 + m_5)$ dependent on the geometry of the system as well as on friction coefficients. These coefficients are evaluated using the actual value of $\sigma(\neq 1)$. The function $\hat{F}$ is defined by $\hat{F} = F/\rho R_c^2\pi$, while $\psi = \rho R_c^2\pi\hat{L}/M$ is the ratio of air mass in the channel to the body mass.

The coefficients κ_c and κ_b measure the pressure drops associated with the channel and body respectively and are in fact the dimensionless pressure drop coefficients associated with the far and near fields. It follows from Eq. (26) that the steady-state† velocity ratio $U_*/V_* \equiv \beta_*$ depends only on the relative magnitudes of these two quantities.

$$\beta_* = 1/(1+\phi), \quad \phi \equiv (\kappa_c/\kappa_b)^{1/2} \quad (28)$$

If the channel is long and the blockage ratio is not too large ($\phi \gg 1$) then $\beta_* \ll 1$, and the fluid is hardly moving. On the other hand, a short, smooth channel and a tightly fitting body will induce fluid velocities that may nearly reach the body velocity itself, in full agreement with intuitive expectations.

In the possession of $U(t)$ and $V(t)$, the total aerodynamic force acting on the body at any instant is easily calculated from the sum of the last three terms in Eq. (17) through multiplication by $\rho R_c^2\pi$. In the simplified theory of this section, the drag is obtained from the second term of Eq. (26) in a similar fashion. We define a drag coefficient, c_D, as

† Star subscripts refer to steady state ($d/dt = 0$).

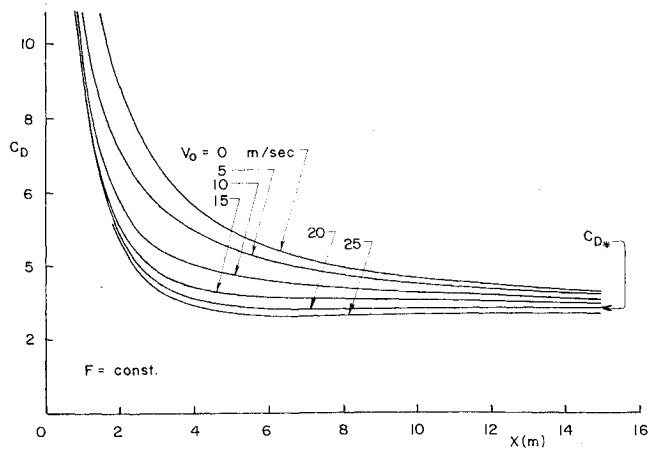

Fig. 6 Variation of c_D along channel for different initial body velocities ($V_0 = 0$). Steady-state drag coefficient indicated by arrow.

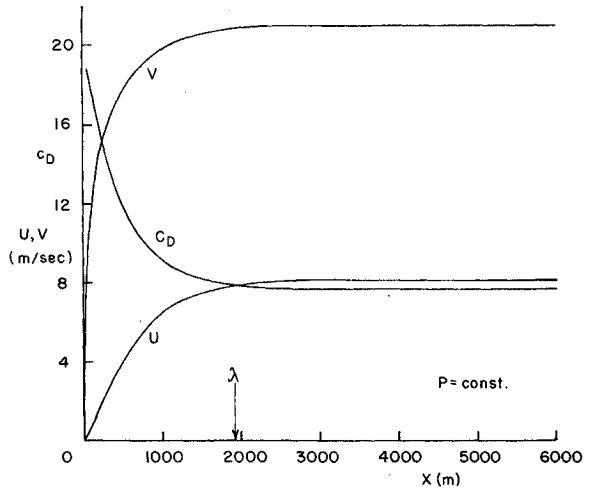

Fig. 7 Variation of V, U, and c_D as functions of body position for full-scale tunnel ($U_0 = V_0 = 0$).

follows:

$$c_D = D/(\tfrac{1}{2}\rho V^2 R_b^2 \pi) \tag{29}$$

Note that c_D in general varies with time: in particular, it decreases for a body accelerating from standstill into an initially quiescent fluid.

Using the simplified model of this section, we can relate c_D to the velocity ratio β in the following form, valid at any instant:

$$c_D = \kappa_b/\sigma(1 - \beta)^2 \tag{30}$$

Specialization to steady-state by using Eq. (28) yields the following remarkable formula:

$$(\sigma c_D{}^*)^{-1/2} = \kappa_b{}^{-1/2} + \kappa_c{}^{-1/2} \tag{31}$$

This equation is clearly valid for any arbitrary propulsive force-velocity relation, i.e., for any function $F(V)$. It shows quite clearly that $c_D{}^*$ depends on both the body and the channel loss coefficients. It is smaller than either of the two coefficients and is principally governed by the *smaller* of the two! This paradoxical result can be illuminated by considering two limiting cases.

1) If $\kappa_b \to 0$, then $c_D{}^* \to 0$, regardless of κ_c. This is entirely sensible, since a friction-free body can slip through the fluid with zero drag, no matter what the fluid velocity (and hence wall drag) is.

2) If $\kappa_c \to 0$, then $c_D{}^* \to 0$, regardless of κ_b. Indeed, if the channel walls are completely frictionless, then the entire fluid mass can be pushed along by the body at no expenditure of power.

In a real case neither coefficient is zero but the trends are easily discerned. If the body is quite tightly fitting (i.e., $\kappa_b > \kappa_c$) then most of the drag is due to the channel walls, so that their surface roughness becomes important. At the same time the body shape loses its significance: a streamlined tail is only marginally superior to a crude, flat end.

On the other hand, the shape of low blockage ratio bodies ($\kappa_b < \kappa_c$) will tend to be crucial, while the smoothness of the channel surface becomes immaterial.

Equation (31) provides a simple relation through which these effects may be quantitatively assessed. This relation clearly shows that one cannot sensibly associate the drag coefficient with the body alone: rather it must be considered as a property of the entire system.

Further headway can be made only after the $F(V)$ function is specified. Two cases will be considered: 1) constant force ($\hat{F}$ = const); and 2) constant power ($\hat{F} = \hat{P}/V$, where $\hat{P} = P/\rho R_c{}^2\pi$, P = propulsive power). The constant force case applies for laboratory drop experiments (Ref. 6) where gravity is utilized as propulsive force in a vertically arranged tube. Constant power, on the other hand, is reasonably representative of real subway situations.

The steady-state body and air velocities are easily calculated for each case by setting the time derivatives equal to zero in Eqs. (26) and (27) and solving the resulting algebraic equations. The results are:

1) Constant force:

$$U_* = \left(\frac{2\hat{F}}{\kappa_c}\right)^{1/2}, \quad V_* = (1 + \phi)\left(\frac{2\hat{F}}{\kappa_c}\right)^{1/2} \tag{32}$$

2) Constant power:

$$U_* = \left(\frac{2\hat{P}}{\kappa_c}\right)^{1/3}(1 + \phi)^{-1/3}, \quad V_* = \left(\frac{2\hat{P}}{\kappa_c}\right)^{1/3}(1 + \phi)^{2/3} \tag{33}$$

The nature of the transient processes can be very conveniently studied if we utilize the fact that the right hand sides of both equations depend on V and U only: time does not appear explicitly. This permits the reduction of this system to one single ordinary differential equation of the first order, simply through the division of Eq. (26) by Eq. (27), resulting in

$$\frac{dU}{dV} = \frac{-\kappa_c U^2 + \kappa_b(V - U)^2}{2\hat{F}(V) - \kappa_b(V - U)^2}\,\psi^{-1} \tag{34}$$

The solutions of this equation can be conveniently examined on a $U(V)$ phase plane by standard methods. The loci of the zero and infinite slopes can be easily found in each case.

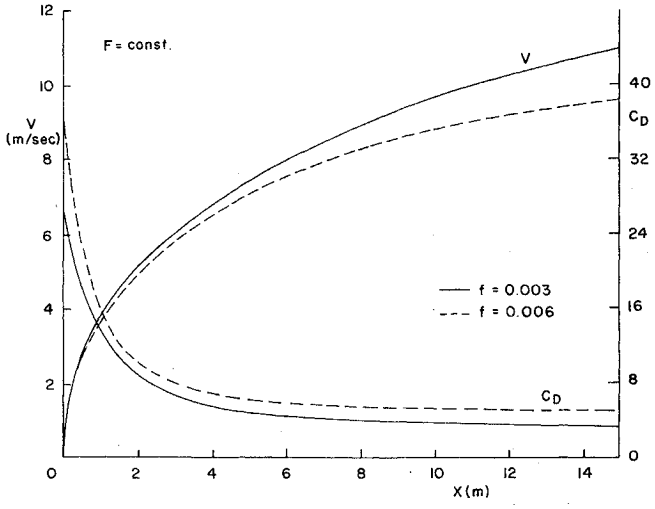

Fig. 8 Effect of friction coefficient on V and c_D. $f = f_c = f_c' = f_b$.

Since they differ only qualitatively, only the constant force case is displayed on Fig. 3. Under the F = const assumption the $dV = 0$ and $dU = 0$ loci are straight lines, intersecting at a singular point specified by Eq. (32). The point can be shown to be a node, so that all solutions will terminate in the steady-state.

Several sample trajectories are shown. Trajectory 1 will occur if the body and fluid are initially at rest. This is the case in gravity-driven experiments, if the body is simply dropped in the tube at the top. Trajectory 2 indicates the consequences of launching the body with a finite velocity into the tube. The body may be temporarily slowed down, only to accelerate again as the fluid is eventually set into motion and thereby the aerodynamic drag is reduced. On the other hand, if the fluid is already flowing fast through the tube when the body is launched, the drag may cause an initial velocity "overshoot" as exemplified by trajectory 3. Several other possible trajectories are also shown.

There is no principal difficulty in performing a phase plane study even if none of the simplifying assumptions of this section are employed, although in the general case the loci of zero and infinite slopes become quadratic curves which are only piecewise continuous. The various possibilities in specifying $F(V)$ and $p_e - p_0$ each lead to a different set of trajectories, the detailed investigation of which is clearly beyond the scope of this paper.

The number of parameters governing the problem is quite large, even in nondimensional form, so that there is no simple, compact form in which all possible solutions could be represented. The main features of the solutions, however, can be described by: 1) the initial conditions; 2) the steady-state values of velocity (U_*, V_*); and 3) by the time and length scales characterizing the adjustment to steady-state. Accurate steady-state velocities can be obtained from Eqs. (17) and (24), after setting the time derivatives to zero. Special problems arise because of the nonanalytical expressions appearing in these equations which render the procedure laborious. Details have been worked out, but will be omitted for brevity. The characteristic time and length scales have been calculated and are given in Ref. 7.

5. Numerical Solutions

The complete equations of Sec. 3 and the simplified equations of Sec. 4 both readily admit numerical integration by computer. Computers can also very easily handle the nonanalytical forms appearing in the equations in Sec. 3. For the sake of easy comparison with the already derived analytical results, we shall again restrict ourselves to the simplified version of the equations.

Figure 4 shows U, V, c_D and t as functions of body position, for conditions typical for an experiment utilizing gravity as a constant propulsion force. The data used for this and all other figures are given in Table 1. The behavior of the solutions corresponds to qualitative expectations. They also demonstrate a fact perhaps not quite foreseen: the system fails to reach a stationary state during the traversing time, and the velocities are still considerably different from their steady-state values when the body leaves the tube. This result is in complete agreement with the estimate of characteristic length scale given in Ref. 7. For the conditions of Fig. 4 this scale turns out to be 4.16 times the channel length, so that it cannot even be indicated on the graph.

The characteristic scale λ is not necessarily longer than the tube although this situation does occur quite often in circumstances of practical interest. Steady state can be reached regardless of the values of $\lambda/\hat{L}$, although the initial conditions may have to be different from $U_0 = V_0 = 0$. Figures 5 and 6 demonstrate how V and c_D vary if $U_0 = 0$, but the body is launched with a finite velocity, i.e., $V_0 \neq 0$. It appears that most solutions correspond to the same large length scale, except the $V_0 = 20$ m/sec case, which reaches virtual steady-state after the remarkably short distance of about 3–4 meters. As discussed in Ref. 7, this phenomenon is due to the existence of exceptional solutions with a shorter than "normal" characteristic distance. If the purpose of the constant force (drop tube) experiment is to realize the particularly interesting steady state situation, then it is mandatory to choose the initial conditions in such a way as to produce this exceptional, fast adjusting behavior.

Figure 6 clearly shows the large values of c_D in the beginning, where a large fraction of the force is used up to accelerate the body and air masses. When the body leaves the tube, the drag coefficients differ from the steady state value by up to 8%, within the range of initial conditions used here. The steady-state value of $c_D{}^*$ is 2.82, which is very much greater than what would be expected in an unconfined stream for an identical slender body.

Figure 7 shows a case representative of a full-scale subway, assuming constant power.‡ Channel area variations, vertical vents and the presence of additional trains were not considered. The figure shows that stationary state is reached, although the distance λ is still sizable, as indicated on the x-axis. In fact, λ may very well be longer than the typical interstation distance, in which case the train would be operating in an unsteady fashion all the time.

The effect of friction factor on the (F = const) solutions is shown on Fig. 8 where $V(x)$ and $c_D(x)$ curves are given for two values of f.

The body speeds are in the ratio of approximately 1.2 to 1 at the time of exit from the tube while the drag coefficients compare as 1.65 to 1. Since for our range of interest $f \sim Re_c{}^{-1/4}$, a factor of two in f corresponds to a factor of 16 in Reynolds number. Model experiments may differ from full-scale train-tunnel systems by two orders of magnitude, so that the present example is representative of scaling problems. The Reynolds number influence is thus not critical, but considerable, and it should be taken into account in the next step of sophistication. This is in principle not difficult in a numerical integration scheme, but greatly hampers analytical studies.

6. Summary and Comments

Equations have been presented which describe the behavior of bodies moving in long channels, as well as the motion of air in the channel as induced by the body. The nature of the solutions have been investigated analytically and numerically.

The examples given concur with previous findings that 1) the drag is considerably increased over what it would be without the confinement of the tunnel and that 2) the power needed to accelerate the air increases the drag over its steady-state value by an increment that may be of the same order as the increase due to confinement alone. Since times required to reach steady-state may be long, this factor must be taken into account in design. Sufficient amount of information is provided to allow the determination of aerodynamic force on the train as well as the air speed in the tunnel under a wide variety of specific circumstances.

An important limitation of the theory stems from the assumption of incompressibility. At higher speeds and larger channel lengths this assumption is clearly not admissible and the theory is increasingly in error. An estimate of the limit of validity may be obtained by requiring that the $p_F - p_R$ pressure difference be small compared to the absolute pressure at the tunnel inlet. In the absence of large heat inputs, this guarantees that the fractional change of density will be also

‡ The P = const assumption yields unrealistic forces at low speeds. This was circumvented by taking $F = F_{\max}$ or $F = P/V$, whichever smaller. $F_{\max}$ was taken to be the force resulting in 0.1 g acceleration of the body. The $F(V)$ relation so defined is an acceptable approximation to real propulsion systems.

small as assumed. The simplified model of Sec. 4 yields

$$p_F - p_R = \tfrac{1}{2}\kappa_b\rho(V_* - U_*)^2 = \tfrac{1}{2}\kappa_c\rho U_*^2 \tag{35}$$

hence, with $p_0 = \rho RT_0$

$$\frac{p_F - p_R}{p_0} = \frac{\gamma\kappa_c}{2}\frac{U_*^2}{\gamma RT_0} = \frac{\gamma}{2}\kappa_c\beta_*^2 M_*^2 \tag{36}$$

where γ is the ratio of specific heats and M^* is the Mach number based on steady-state train speed and inlet acoustic velocity. We arbitrarily designate $(p_F - p_R)/p_0 = 0.1$ as a highest tolerable value of pressure change and call the associated Mach number M_{cr}. Using Eqs. (28, 31 and 36), we then have

$$M_{cr} = 0.374\ (\sigma c_{D*})^{-1/2} \tag{37}$$

where we set $\gamma = 1.4$. If the train Mach number is less than M_{cr}, the pressure drop across the train is less than 10% of p_0 and the present theory should be a reasonably good approximation.

As an example, we may take the case of Fig. 7 (see Table 1 for details) and find $M_{cr} = 0.27$. This means that the theory of this paper should yield acceptable results if the train speed is less than approximately 200 mph, which is probably true for all systems presently operating or under design. Note however, that increasing blockage ratios and increasing tunnel lengths may quickly render compressibility effects important.

Table 1 Data for Numerical Examples

Quantity	Dimension	Figs. 4, 5, 6, 8	Fig. 7
L	m	15.39	6,000.
$2R_c$	m	0.05291	4.877
l_b	m	0.4557	90.
$2R_b$	m	0.04475	3.448
$f_c = f_c' = f_b$	—	0.003 (also 0.006 on Fig. 8)	0.005
$\zeta_0^+ = \zeta_F^+$	—	1.0	1.0
$\zeta_e^+ = \zeta_R^+$	—	0.0	0.0
F	Newton	0.04758	—
P	Watt	—	1.76×10^6
M	kg	0.0485	0.124×10^6
ρ	kg/m³	1.205	1.205
	Derived Quantities		
σ	—	0.7153	0.5
ψ	—	0.8157	4.35
κ_c	—	4.388	25.61
κ_b	...	19.42	10.13
$\hat{F}$	(m/sec)²	179.6	...
$\hat{P}$	(m/sec)³	—	19.55×10^3

Another major simplification resulted from assuming fluid friction to be Reynolds number independent. The insight gained from the consequent simplicity amply justifies the assumption, but renders quantitative predictions questionable. A body accelerating from standstill passes through the entire Reynolds number range from zero to the maximum value in times that are shorter or comparable to times required for the development of the boundary layers in the far field. The flow development thus cannot be considered as a quasi-stationary process and it is not legitimate to use the conventional (steady-state) pipe friction factors evaluated at the instantaneous Reynolds number. In laboratory experiments, where the initial conditions may be made truly quiescent, a laminar-turbulent transition will occur which clearly influences the drag. In real subways the upstream conditions are greatly disturbed by previous trains and the flow may be quite dependent on this kind of turbulence.

It would be desirable to extend the work on this topic in several directions. In addition to the air speed, it is of interest to know the air temperature as a function of location and time, for purposes of climate control design and passenger comfort. The role of segments of different cross sections in the channel (stations) and of vertical ventilation shafts in determining drag and air speed are of interest. Interaction of several trains simultaneously moving in the channel is a practical problem. It would be interesting and quite feasible to simulate a complete system by computer: the power needs of each train for a prescribed schedule of operation could be determined and so could the resultant air motion and temperature distribution throughout the entire system. Finally, compressibility effects in unsteady operation might be considered and aerodynamic means of propulsion are worthy of study.

References

[1] Hara, T., "Aerodynamic Drag of Trains in Tunnels," *Quarterly Report of Railway Technical Research Institute*, Vol. 8, Japan, 1967, pp. 229–235.

[2] Hammitt, A. G., Hersh, A. S., Murthy, K. R. A., Peterson, J. B., and Bliss, D. B., "Drag of Vehicles Traveling in Tubes," AIAA Paper 68-160, New York, 1968.

[3] Schlichting, H., *Boundary Layer Theory*, 4th ed., McGraw-Hill, New York, 1960, pp. 521, 523, 531.

[4] Davis, H. T., *Introduction to Nonlinear Differential and Integral Equations*, Dover, New York, 1962.

[5] Gouse, S. W. Jr., Noyes, B. S., Nwude, J. K., and Swarden, M. C., Aerodynamic Drag on Vehicles in Tunnels, *Journal of Basic Engineering*, Vol. 91, 1969, pp. 694–706.

[6] Dayman, B. Jr., "Considerations for Design and Operation of Facilities to Measure Aerodynamics of Vehicles Traveling in Tubes," AIAA Paper 70-225, New York, 1970.

[7] Sajben, M., "Fluid Mechanics of Train-Tunnel Systems in Unsteady Motion," AIAA Paper 70-141, New York, 1970.